

Growth on Differently Oriented Sidewalls of SiC Mesas As a Way of Achieving Well-Aligned SiC Nanowires

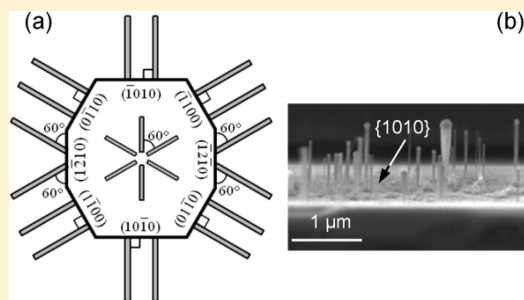
Rooban Venkatesh K. G. Thirumalai,[†] Bharat Krishnan,[†] Albert V. Davydov,[‡] J. Neil Merrett,[§] and Yaroslav Koshka^{*†}

[†]Department of Electrical and Computer Engineering, Mississippi State University, Mississippi State, Mississippi 39762, United States

[‡]National Institute of Standards and Technology, Gaithersburg, Maryland 20899, United States

[§]Air Force Research Laboratory, Wright-Patterson Air Force Base, Ohio 45433, United States

ABSTRACT: Several different growth directions of SiC nanowires (NWs) determined by the substrate surface crystallographic orientation were achieved by conducting vapor–liquid–solid growth on the top surfaces and the sidewalls of the 4H-SiC mesas. When substrate-dependent (i.e., epitaxial) growth was ensured, six possible crystallographic orientations of 3C-SiC NW axis with respect to the 4H-SiC substrate were realized. They all were at 20° with respect to the substrate *c* plane, and their projections on the *c* plane corresponded to one of the six equivalent $\langle 10\bar{1}0 \rangle$ crystallographic directions. All six orientations were obtained simultaneously when growing on the (0001) top surface of the 4H-SiC wafer or on the mesa tops. In contrast, no more than two NW orientations coexisted when grown on any particular crystallographic plane of a mesa sidewall. In particular, the $\{10\bar{1}0\}$ mesa sidewall plane resulted in only one NW orientation, thereby producing well-aligned NW arrays desirable for device applications.



INTRODUCTION

Semiconductor nanowires (NWs) are currently among the most explored research directions in nanotechnology, with the most interesting applications anticipated in the biomedical field.¹ While NWs of many different semiconductor materials are being currently investigated, silicon carbide (SiC) NWs are attractive because of the wide band gap of this material, its high breakdown strength, and radiation resistance, and it is one of the best mechanical strengths and thermal conductivity of all semiconductors.² Furthermore, impressive chemical stability and strong evidence of good biocompatibility of SiC^{3–5} make SiC NWs very promising for biomedical applications and for gas-sensing in harsh environments.^{6,7}

Chemical vapor deposition (CVD) is a promising technique to grow NWs of SiC with controlled polytype,^{8–10} compared to other techniques attempted so far. Various substrates were used for SiC NW synthesis, including SiO₂,^{10–12} graphite,^{13–16} and poly-SiC.⁸ Use of polycrystalline or amorphous substrates naturally provides a nonepitaxial growth mechanism for SiC NWs, which commonly crystallize in the 3C polytype. Reported crystallographic orientations of the 3C NW axis include $\langle 111 \rangle$ ^{10–15} as well as more rare observations of $\langle 110 \rangle$, $\langle 100 \rangle$, and $\langle 112 \rangle$.⁹ Other SiC polytypes, when growing on substrates other than monocrystalline SiC, were occasionally obtained including 6H,^{8,13,14} 2H,^{8,11} and 15R.^{8,16} Only a few studies have reported traces of the 4H polytype when using substrates other than monocrystalline SiC.^{16,17}

Use of monocrystalline 4H- and 6H-SiC substrates was recently motivated by the desire to achieve polytype reproducibility from the substrate to the NWs.^{18–20} While

some evidence for the dominance of the 6H polytype in NWs grown on 6H-SiC substrate was provided in ref 18, it remains challenging to achieve single-polytype NWs that replicate the polytype of the substrate. However, the observed alignment of the NW axes along only a few certain orientations dictated by the SiC substrate^{18,20} indicated that the epitaxial growth mode was achieved. Besides providing a promising avenue to achieving polytype reproducibility, the use of monocrystalline SiC substrates could be the most reliable approach to fabricating well-aligned parallel NWs by the bottom-up approach, which is desirable for many nanoelectronic and sensor applications.

In our previous work, the epitaxial growth mode for 3C-SiC NWs was investigated on the (0001) growth surface of the 4H-SiC substrate.²⁰ Six preferential orientations of the NW axis with respect to the substrate were obtained. They all were at 20° with respect to the substrate *c*-plane and their projections on the *c* plane corresponded to one of the six equivalent $\langle 10\bar{1}0 \rangle$ crystallographic directions. In this work, growth on differently oriented walls of 4H-SiC mesas is investigated. A possibility to obtain well-aligned SiC NWs by choosing proper crystallographic orientations of the growth surface is explored.

EXPERIMENTAL SECTION

SiC NW growth experiments were conducted in a hot-wall CVD reactor at 150 Torr with H₂ as the carrier gas and SiCl₄ and CH₃Cl as

Received: October 21, 2011

Revised: February 29, 2012

Published: March 20, 2012



the silicon and carbon sources, respectively.²⁰ Pieces of commercial heavily doped n-type 4H-SiC (0001) wafers vicinally cut 8° toward the [11 $\bar{2}$ 0] direction were used as the growth substrates. Rectangular and circular 4H-SiC mesas of varying dimensions were formed by reactive ion etching with a 9:1 ratio of SF₆/O₂ at 70 mTorr using Ni as an etch mask. Resulting mesa heights were between 10 and 17 μm tall (Figure

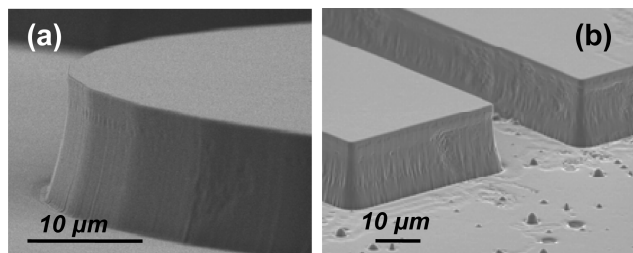


Figure 1. (a) Circular and (b) rectangular mesas formed on 4H-SiC substrates, formed to be used for vapor–liquid–solid growth of SiC NWs.

1). A four hour dry oxidation was performed at 1100 °C and then removed in a buffered HF solution. Etching of the mesa surfaces in H₂ ambient at 1500 °C was conducted prior to using them for the NW growth to reduce surface roughness, which could serve as heterogeneous nucleation sites for the NW growth. Hydrogen etching duration was varied between 15 and 20 min depending on the initial mesa surface roughness. Improvement in the surface roughness was examined using SEM. Temperature was ramped at a rate of 118 °C/min and held at 1500 °C with hydrogen flow of 10 L/min for the entire etching duration.

The metal catalyst for the vapor–liquid–solid (VLS) NW growth was delivered to the growth surfaces in situ by the vapor-phase catalyst delivery mechanism.²¹ Either a separate catalyst-source substrate covered with a blanket-deposited layer of NiSi or NiSi regions patterned on the surface of the SiC growth-substrates were used. The NiSi layers with thicknesses around 2000 Å thick were deposited by sputtering in Ar from a NiSi target. The patterned NiSi layers were formed by using a conventional lift-off photolithography technique.

The samples were then cleaned by ultrasonic shaking in acetone, isopropanol, and DI water before the growth run. The samples were then placed inside the opening of the hot-wall susceptor in the reactor. The catalyst source (a small piece of a substrate covered with NiSi) was normally placed 1–2 mm upstream from the sample. After establishing the target pressure in the H₂ flow, the temperature was ramped to 1150 °C in 10–15 min. The growth run was initiated by establishing the desired flows of the silicon and carbon precursor. On the basis of the NW length obtained after a 30 min run at 1150 °C, the growth time was adjusted to obtain a desired NW length most convenient for investigating the growth orientation.

The NWs were characterized by Nomarski optical microscopy, X-ray diffraction (XRD), and scanning electron microscopy (SEM) equipped with electron backscatter diffraction (EBSD). The latter method was used to identify polytypes of the individual NWs growing on particular mesa walls. The EBSD patterns were recorded using an HKL Nordlys II EBSD detector attached to the Hitachi S-4700 microscope.

RESULTS AND DISCUSSION

Experimental parameters including growth temperature, catalyst source and its thickness, and the flows of the growth precursors were varied to find the most favorable conditions for growing NWs with low density on the substrate, which are the most convenient for investigating the preferential growth orientations. A NiSi catalyst delivered to the growth surface by the vapor-phase catalyst delivery mechanism²¹ provided the easiest way of achieving low NW density. Furthermore, the use

of the vapor-phase catalyst delivery method allowed growing on all available planes of the patterned SiC substrate, including the vertical sidewalls of the SiC mesas.

As follows from ref 21, surface damage caused by RIE may dramatically enhance heterogeneous nucleation of the metal catalyst and cause undesirably high density of SiC NWs. To achieve sufficiently low density of NWs on the mesa surfaces, H₂ etching of the SiC substrates at 1500 °C for 10 min was conducted prior to the NW growth. The etching time and the temperature selected are estimated to remove 0.2 to 0.3 μm of the SiC thickness from the top surface of the mesa;²² other crystallographic planes may etch at a significantly higher rate. In any case, mesa sidewalls predominantly free from visible surface defects were achieved after the H₂ etching (Figure 1).

Figure 2a shows a schematic projection of NW orientations onto the substrate (10 $\bar{1}$ 0) plane, which were observed

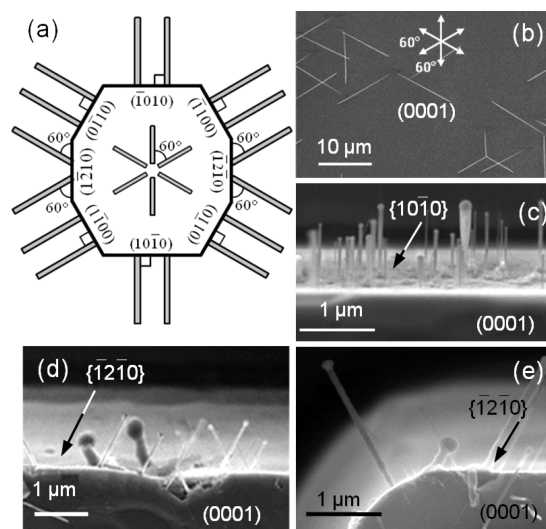


Figure 2. Top view of SiC NWs growing on the top surface and the vertical sidewalls of SiC mesas: (a) a schematic showing azimuth orientation of the growth direction, (b) an SEM image of NWs growing on (0001) surface, (c,d) NWs growing on {10 $\bar{1}$ 0} and {1 $\bar{2}$ 10} planes, respectively, (e) simultaneous NWs growing on (0001) surface, a { $\bar{1}$ 2 $\bar{1}$ 0} plane and on the rounded edge of the mesa representing a gradual transition from {1 $\bar{2}$ 10} to {10 $\bar{1}$ 0}.

experimentally in Figure 2b–e. Similar to our previous work investigating growth on unpatterned (0001) 4H-SiC surfaces,²¹ the NWs on the top (0001) surfaces of the SiC mesas grew along six directions (Figure 2a,b). They all formed 20° angle with the *c* plane of the substrate (Figure 3), and their projections on the *c* plane corresponded to one of the six

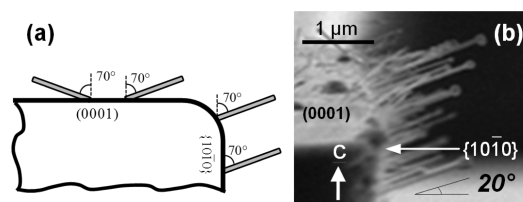


Figure 3. Side view demonstrating the growth angle of the NWs with respect to the *c* axis: (a) a growth schematic and (b) an SEM image of NWs growing on the vertical sidewalls of a SiC mesa, confirming the 70° angle with respect to the *c* axis (20° angle with respect to the basal plane).

equivalent $\langle 10\bar{1}0 \rangle$ crystallographic directions (i.e., the projections are aligned at 60° with respect to each other).

It should be noted that the 20° is the angle with respect to the basal plane of the substrate, which was calculated from the angle between the NW axis and the surface by accounting for the surface off-axis angle. The same 20° angle to the c plane was observed for all six NW axis directions.

Next, the NW growth was investigated on vertical mesa sidewalls having a wide range of crystallographic orientations, which were provided by circular mesas and the rounded edges of the rectangular mesas. Notably, the same six orientations of the NW axes and no other orientations were observed when growing on vertical mesa sidewalls as illustrated in Figure 2a.

The top-down SEM view was used for evaluating the angle of the NW projections on the c plane. The use of any particular $\{10\bar{1}0\}$ mesa sidewall plane resulted in only one corresponding NW orientation, wherein the NW projection on the c axis was perpendicular to the corresponding $\{10\bar{1}0\}$ plane (Figure 2a,c).

Two different NW orientations often coexisted when growing on any particular $\{12\bar{1}0\}$ mesa sidewall. Projection of any of those NWs on the c plane still corresponded to one of the six orientations observed on the top (0001) surface as discussed above (Figure 2a,d). Furthermore, mesa sidewalls corresponding to a transition from $\{10\bar{1}0\}$ to $\{12\bar{1}0\}$ crystallographic planes still exhibited a maximum of two NW orientations (see, for example, the rounded mesa edge in Figure 2e).

However, the NWs on $\{10\bar{1}0\}$ mesa sidewall planes were not perpendicular to the corresponding planes. In fact, all NWs formed a 70° angle with the c axis (i.e., 20° angle with the c plane), which is the same angle as that of the NWs growing on the (0001) surface (Figure 3). Only this angle with respect to the c -plane could be observed when growing on any other vertical sidewall plane as well as on any of the rounded mesa edges or the rounded edges of the SiC substrates representing all possible planes when observing a transition from (0001) top surface to the vertical sidewall planes (Figure 4). Furthermore,

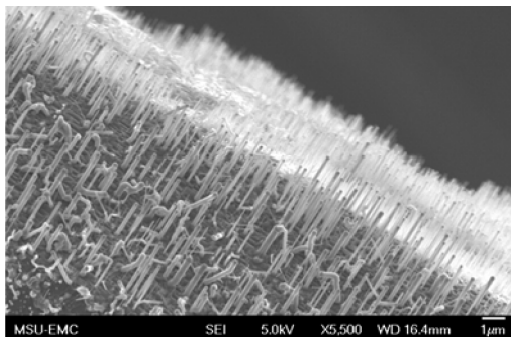


Figure 4. Aligned SiC NWs growing on the $\{10\bar{1}0\}$ plane of the SiC substrate and across the rounded edge corresponding to the transition from (0001) substrate surface to the $\{10\bar{1}0\}$ plane (see the schematic diagram of Figure 3a).

growth on the rounded edges corresponding to the transition from the (0001) plane to the $\{10\bar{1}0\}$ vertical sidewalls resulted in a single orientation of the NW axes (Figure 4), thereby providing only well-aligned parallel NWs grown in the particular location.

XRD and high-resolution TEM measurements on samples with sufficiently high density of the NWs and high-resolution TEM measurements showed domination of 3C NWs with their

growth axis corresponding to the $\langle 111 \rangle$ direction.²⁰ Since those techniques did not allow us to reliably establish if the characterization data correspond to the NWs grown on the top surface or the vertical sidewalls of the mesas, EBSD measurements targeting individual NWs grown on the vertical sidewall (Figure 5) were used to supplement the XRD and TEM results.

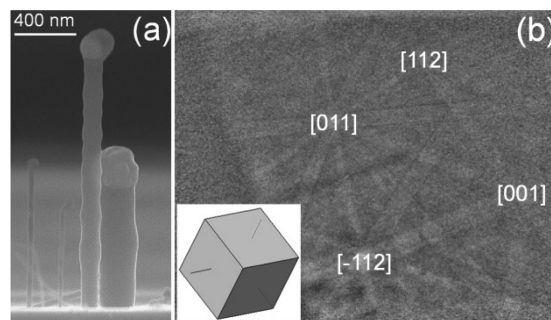


Figure 5. (a) SEM of 3C-SiC NWs growing on $\{10\bar{1}0\}$ surface and (b) corresponding EBSD pattern with simulated crystallographic orientation of the 3C unit cell in the inset.

For statistical validity, EBSD patterns from multiple NWs that grew on the mesa top surfaces and on sidewalls were analyzed using crystallographic data for most common SiC polytypes, including 3C, 2H, 4H, and 6H. Only 3C phase indexing produced a consistent and accurate match to the experimental diffraction results. The example in Figure 5b shows the example of 3C indexing of EBSD from a NW that grew on the $\{10\bar{1}0\}$ sidewall. However, since NWs grew at various angles with respect to both the top and the side substrate facets and, therefore, their absolute orientation in the EBSD geometry setup was not unequivocal, it was difficult to reliably determine their growth axis. A previous TEM study of random 3C-SiC NWs from the same set showed the growth axis to be $\langle 111 \rangle$.²¹ Therefore, using the combination of the TEM²¹ and the EBSD results from this work, it was concluded that all 3C-SiC NWs that grew along one of the six directions with respect to the substrate had their growth axes along the $\langle 111 \rangle$ crystallographic direction.

As discussed in ref 20, when 3C NWs with $[111]$ axis grow at 70° angle with respect to the c axis, this results in the $\{\bar{1}11\}$ plane (which is also the plane for the SF in the 3C-SiC NWs) being parallel to the basal plane of the substrate. In addition, since the NW projection on the (0001) plane points along one of the six equivalent $\langle 10\bar{1}0 \rangle$ crystallographic directions, it is unambiguous that the $\{112\}$ and $\{110\}$ planes in 3C NWs are parallel to the $\{10\bar{1}0\}$ and $\{11\bar{2}0\}$ planes of the 4H substrate, respectively. It is suggested that this orientation relationship yields the best lattice match between 3C NWs and the 4H (0001) substrate. This result agrees with the epitaxial relationship between the 3C-SiC inclusions and the 4H-SiC matrix and between the 3C films and the hexagonal SiC surfaces used for the 3C heteroepitaxial growth.^{23,24} Also, as illustrated by schematic atomic alignment in Figure 6, it provides a very small in-plane lattice mismatch of 0.2% between 3C- and 4H-SiC. Noteworthy, this lattice alignment is the same as for the epitaxial growth of hexagonal $\langle 0001 \rangle$ oriented GaN NWs on a cubic Si(111) substrate.²⁵

It follows from the experimental results of this work that the same alignment of the 3C and 4H lattices (i.e., the same

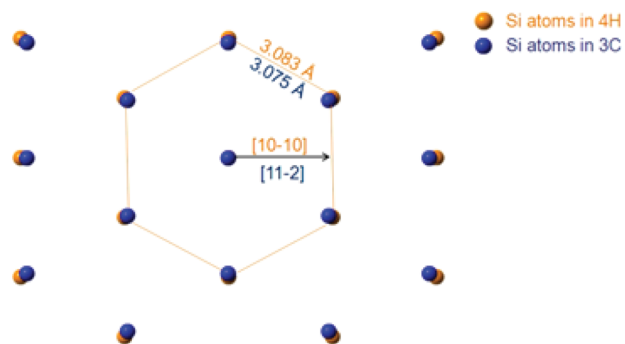


Figure 6. Atomic arrangement of 3C (111) plane on 4H (0001) plane with the following epitaxial relationships: (111) 3C|| (0001) 4H and $[11\bar{2}]$ 3C|| $[10\bar{1}0]$ 4H. Note that a very small in-plane lattice mismatch of 0.2% was calculated using 3C and 4H lattice parameters.

epitaxial relationship) is preserved when the heteroepitaxial NW growth is conducted on other planes of the 4H-SiC substrate, i.e., the {111} NW plane becomes parallel to the (0001) substrate plane and the {112} NW plane becomes parallel to the $\{10\bar{1}0\}$ substrate plane. Specifically, when NWs grow on the $\{10\bar{1}0\}$ sidewall (see Figure 2c), the NW/substrate interface likely lies in the (112) plane of the 3C structure, while NWs that grew on the $(11\bar{2}0)$ sidewall (Figure 2d) are attached by their (110) planes. When the growth is conducted on the out-of-plane surfaces (i.e., mesa surfaces corresponding to a transition between the main crystallographic orientations discussed above), the same epitaxial relationship between the lattices of the substrate and NWs was preserved.

When turning the discussion from the relative orientation of the crystal lattices of the NWs with respect to the substrate to the orientations of the NW axes, it may look surprising that the growth on vertical sidewalls also resulted in NWs having their axes pointing along one of the same six orientations with respect to the substrate as what happened when growing on the (0001) top substrate surface. However, considering the same alignment of the crystal lattices regardless of the growth surface, this result only means that all the 3C NWs have $\langle 111 \rangle$ growth axis. For example, for the same relative orientation of the lattices of the NWs and the substrate, the $\langle 112 \rangle$ cubic orientation of the NW axis would be perpendicular to the $\{10\bar{1}0\}$ plane of the substrate, etc. While $\langle 112 \rangle$ axes have been occasionally reported for 3C SiC NWs,⁹ the $\langle 111 \rangle$ direction seems to be more energetically favorable for most of the growth conditions reported in the literature, which could possibly be due to minimization of the NW surface energy for this particular crystallographic orientation.

The NW axis orientations for 3C NWs grown on hexagonal SiC substrates established in this work are different from those reported for 6H NWs grown on 6H substrates.¹⁸ In ref 18, 6H NWs grew along the six equivalent $[\bar{1}102]$ directions on SiC (0001) substrates (which corresponds to the top mesa surface in the present work) and along the other six equivalent $[10\bar{1}0]$ directions on SiC $(10\bar{1}0)$ and $(11\bar{2}0)$ substrates (which corresponds to the vertical mesa sidewalls in the present work). In the present work, only six orientations of 3C NWs could be observed on all investigated surfaces (i.e., the axes of 3C NWs are not in the c plane when growing on the vertical sidewalls). Accidentally, the 20° angle with respect to the substrate c plane was observed in both the experiments of this work and in ref 18. However, while the 20° angle corresponds to $[\bar{1}102]$ directions in the 6H substrate, in 4H-SiC, this angle

does not correspond to any of the low-index directions. The same heteroepitaxial relationship should be expected when growing 3C NWs on the (0001) plane of 6H substrates, which means that both 3C $[111]$ NWs and 6H $[\bar{1}102]$ NWs would have the same orientations of their axes. In contrast, growing 4H NWs on 4H substrate with their growth axes along $[\bar{1}102]$ direction would correspond to $\sim 60^\circ$ (rather than 70°) angle to the c plane of the substrate.

CONCLUSIONS

The two main results of this work are (1) a demonstration that the growth of 3C-SiC NWs on different surfaces of 4H-SiC substrates by CVD is governed by the epitaxial growth mechanism where the (111) NW plane is parallel to the (0001) plane of the substrate and the (112) NW plane is parallel to the $(10\bar{1}0)$ plane of the substrate; and (2) development of a method for fabricating arrays of well-aligned (i.e., all-parallel) 3C-SiC NWs by the bottom-up approach, which is accomplished by epitaxial growth on crystallographically selected growth surfaces. While as many as six different orientations of the NW axes (i.e., six equivalent $\langle 10\bar{1}0 \rangle$ crystallographic directions with respect to the substrate lattice) are possible when growing on the (0001) surface, growth on the $\{10\bar{1}0\}$ surfaces as well as on the surfaces that are transitional from (0001) to $\{10\bar{1}0\}$ provides only a single orientation of the 3C-SiC NWs for the particular growth surface.

When using commercial (0001) 4H-SiC substrates, the $\{10\bar{1}0\}$ surface planes are provided by some of the vertical sidewalls of the mesas formed on the top substrate surface. This enables the growth of well-aligned close-to-horizontal NW arrays (more precisely, 20° inclined with respect to the substrate surface ignoring a possible off-cut angle), which is convenient for device fabrication using conventional planar lithography.

AUTHOR INFORMATION

Corresponding Author

*E-mail: ykoshka@ece.msstate.edu.

Notes

The authors declare no competing financial interest.

REFERENCES

- (1) Stern, E.; Vacic, A.; Reed, M. A. *IEEE Trans. Electron Devices* **2008**, *55* (11), 3119–3130.
- (2) Zekentes, K.; Rogdakis, K. *J. Phys. D: Appl. Phys.* **2011**, *44* (13), 133001.
- (3) Li, X.; Wang, X.; Bondokov, R.; Morris, J.; An, Y. H.; Sudarshan, T. S. *J. Biomed. Mater. Res., Part B* **2005**, *72* (2), 353–61.
- (4) Santavirta, S.; Takagi, M.; Nordstletten, L.; Anttila, A.; Lappalainen, R.; Konttinen, Y. T. *J. Biomater. Appl.* **1998**, *118*, 89–91.
- (5) Sadow, S. E.; Coletti, C.; Frewin, C.; Schettini, N. C.; Oliveros, A.; Jaroszeski, M. *Mater. Res. Soc. Symp. Proc.* **2010**, *1246*, 193–198.
- (6) Yakimova, R.; Petoral, R. M., Jr.; Yazdi, G. R.; Vahlberg, C.; Lloyd Spetz, A.; Uvdal, K. *J. Phys. D: Appl. Phys.* **2007**, *40* (20), 6435–6442.
- (7) Neudeck, P. G.; Spry, D. J.; Trunek, A. J.; Evans, L. J.; Chen, L.-Y.; Hunter, G. W.; Androjna, D. *Mater. Sci. Forum* **2009**, *600–603*, 1199–1202.
- (8) Pampuch, R.; Gorny, G.; Stobierski, L. *Glass Phys. Chem.* **2005**, *31* (3), 370–376.
- (9) Peng, H. Y.; Zhou, X. T.; Lai, H. L.; Wang, N.; Lee, S. T. *J. Mater. Res.* **2000**, *15* (9), 2020–2026.
- (10) Seong, H.-K.; Park, T. E.; Lee, S. C.; Lee, K. R.; Park, J. K.; Choi, H. *J. Met. Mater. Int.* **2009**, *15* (1), 107–111.

- (11) Yao, Y.; Lee, S. T.; Li, F. H. *Chem. Phys. Lett.* **2003**, *381* (5–6), 628–633.
- (12) Seong, H.-K.; Choi, H.-J.; Lee, S.-K.; Lee, J.-I.; Choi, D.-J. *App. Phys. Lett.* **2004**, *85* (7), 1256.
- (13) Wang, H.; Xie, Z.; Yang, W.; Fang, J.; An, L. *Cryst. Growth Des.* **2008**, *8* (11), 3893–3896.
- (14) Gao, F.; Yang, W.; Wang, H.; Fan, Y.; Xie, Z.; An, L. *Cryst. Growth Des.* **2008**, *8* (5), 1461–1464.
- (15) Wu, R.; Li, B.; Gao, M.; Chen, J.; Zhu, Q.; Pan, Y. *Nanotechnology* **2008**, *19* (33), 335602.
- (16) Bechelany, M.; Brioude, A.; Cornu, D.; Ferro, G.; Miele, P. *Adv. Funct. Mater.* **2007**, *17* (6), 939–943.
- (17) Yoshida, H.; Kohno, H.; Ichikawa, S.; Akita, T.; Takeda, S. *Mater. Lett.* **2007**, *61* (14–15), 3134–3137.
- (18) Wang, H.; Lin, L.; Yang, W.; Xie, Z.; An, L. *J. Phys. Chem. C* **2010**, *114* (6), 2591–2594.
- (19) Sundaresan, S. G.; Davydov, A. V.; Vaudin, M. D.; Levin, I. *Chem. Mater.* **2007**, *19* (23), 5531–5537.
- (20) Krishnan, B.; K. G. Thirumalai, R. V.; Koshka, Y.; Sundaresan, S.; Levin, I.; Davydov, A. V.; Merrett, J. N. *Cryst. Growth Des.* **2011**, *11* (2), 538–541.
- (21) K. G. Thirumalai, R. V.; Krishnan, B.; Davydov, A. V.; Merrett, J. N.; Koshka, Y. *Nanotechnology*, to be published in Journal of Materials Research.
- (22) Zhang, J.; Kordina, O.; Ellison, A.; Janzén, E. *Mater. Sci. Forum* **2002**, *389–393*, 239–242.
- (23) Si, W.; Dudley, M.; Kong, H. S.; Sumakeris, J.; Carter, C., Jr. *J. Electron. Mater.* **1997**, *26* (3), 151–159.
- (24) Latu-Romain, L.; Chaussende, D.; Pons, M. *Cryst. Growth Des.* **2006**, *6* (12), 2788–2794.
- (25) Landré, O.; Songmuang, R.; Renard, J.; Bellet-Amalric, E.; Renevier, H.; Daudin, B. *Appl. Phys. Lett.* **2008**, *93* (18), 183109.